Design of a Rotating Test Rig for Transient Thermochromic Liquid Crystal Heat Transfer Experiments

Christian Waidmann, Rico Poser, Sven Nieland, Jens Von Wolfersdorf

Design of a Rotating Test Rig for Transient Thermochromic Liquid Crystal Heat Transfer Experiments

Christian Waidmann[1]*, Rico Poser[1], Sven Nieland[1], Jens von Wolfersdorf[1]

ISROMAC 2016

International Symposium on Transport Phenomena and Dynamics of Rotating Machinery

Hawaii, Honolulu

April 10-15, 2016

Abstract

The design of a test rig for the investigation of turbine blade internal cooling channel configurations under the influence of rotation is presented. Rotational speeds of up to 900 rpm in combination with the possibility to operate the test model with fluid pressures of up to 10 bar and fluid temperatures between -100 °C and +80 °C provide a wide range of achievable test conditions. The rig will be used to study the effect of Coriolis forces and buoyancy forces on heat transfer distribution in internal cooling channels.

The transient thermochromic liquid crystal (TLC) technique will be used to obtain spatially resolved heat transfer measurements. This method evaluates the TLC colorplay on heat transfer surfaces resulting from a fluid temperature change. The air supply system to the test model and the approach to induce the required fluid temperature change is described. A preliminary non-rotating test rig was set-up to investigate the achievable fluid temperature change.

Stationary video cameras and strobe lamps will be installed to capture the TLC colorplay. Preliminary tests have been conducted to test the synchronization of the cameras and strobe lamps with the rotational speed. The strobe flash stability and the possibility of interfering motion blur effects have been evaluated.

Keywords

Heat Transfer — Thermochromic Liquid Crystal — Turbine Blade — Rotating Effects

[1] *Institute of Aerospace Thermodynamics, University of Stuttgart, 70569 Stuttgart, Germany*

***Corresponding author**: christian.waidmann@itlr.uni-stuttgart.de

INTRODUCTION

Heat transfer can significantly differ between a non-rotating and a rotating cooling channel. Coriolis forces and rotational buoyancy forces in a rotating cooling channel induce secondary flows which alter the flow structure and thus the heat transfer distribution at the channel walls. Both forces have also an impact on the turbulence field.

Rotation can significantly increase the spreading of heat transfer coefficients. Thus, heat transfer can be enhanced on one channel wall and at the same time drastically reduced on the opposite wall, depending on the flow direction and direction of rotation. For the design of advanced cooling channel geometries with a reduced cooling air consumption, it becomes more and more important to understand and assess the influence of rotation. Hence, an increasing number of research facilities apply rotating test rigs for experimental studies.

Wagner et al. [1] investigated the effects of rotation on heat transfer in turbine blade internal coolant passages with smooth walls and varied coolant density ratio, Rotation number, Reynolds number and radius ratio. They observed increases in heat transfer of up to a factor of 3.5 on the trailing surfaces and decreases down to 40 percent on the leading surfaces compared to non-rotating conditions, for a channel with radial outward flow. In this investigation individually heated cooper segments were applied and tailored to achieve a constant wall temperature. The segment-averaged data provide information for a wide range of operating conditions but lack local resolution.

Using a multipass, smooth-wall heat transfer model Wagner et al. [2] found that the effect of rotation on heat transfer coefficients is considerably different depending on the flow direction. Blair et al. [3] described the application of a transient TLC technique for a rotating test rig. The TLC information can provide more local details and were monitored with a stationary camera-setup similar to the concept considered here. Morris [4] described the design philosophy for the development of a rotating research facility. He listed cooling channel parameters for typical real engine conditions and presented the non-dimensional groups that are used to simulate these conditions in a laboratory setup.

Davenport [5] presented a rotating test rig capable of rotating speeds of up to 4000 rpm. He also applied the TLC technique and used cameras and LED lighting that are incorporated into the rotating test model. Therewith time-synchronization between stationary cameras and TLC-data in the rotating model can be avoided. The incorporation of cameras and lighting into the rotating model and the associated energy supply and data storage, however, is a difficult challenge.

Therefore, a concept with stationary cameras and strobe lighting has been chosen for a new test rig that is currently being set up at the Institute of Aerospace Thermodynamics (ITLR) at the University of Stuttgart. The test rig will be used to investigate engine-similar turbine blade cooling geometries under the influence of rotation.

The transient thermochromic liquid crystal technique will be applied to obtain spatially resolved heat transfer measurements [6]. For this technique optical access to the TLC-coated

channel walls is required. Therefore, the cooling channel geometry is manufactured out of Perspex. The test model will be mounted inside an aluminum housing at the end of the rotor arm at a mean model radius of 750 mm. Cooling air will be supplied to the model through insulated pipes inside the hollow shaft and the hollow rotor arm.

Rotational speeds of up to 900 rpm in combination with fluid pressures of up to 10 bar are planned to provide a wide range of achievable test conditions.

To validate the concept of the test rig, preliminary tests have been conducted to investigate particular measurement aspects. A non-rotating preliminary test rig with comparable air supply passages has been set up to assess the achievable temperature change that is required for the TLC tests. Furthermore, preliminary rotating tests have been conducted to validate the synchronization of a stationary camera and strobe light with the speed of a rotating disc. Test patterns on the disc allowed to evaluate motion blur effects.

NOMENCLATURE

η	Dynamic viscosity
ρ	Density of fluid
λ_f	Thermal conductivity of fluid
Ω	Rotational speed [rad/s]
A	Cross-section area of channel
Bo	Buoyancy number
d_h	Hydraulic diameter
E	Mean intensity of reference pixel group
h	Heat transfer coefficient
I	Intensity [gray-scale value]
j	Video frame number
Ma	Mach number
$\dot{m}$	Mass flow rate
N	Total number of video frames
Nu	Nusselt number
Pr	Prandtl number
R	Model radius
Re	Reynolds number
Ro	Rotation number
T	Fluid temperature
$T1\_IN$	Temp. of primary test air at valve unit inlet
$T1\_OUT$	Temp. of primary test air at valve unit outlet
$T2\_IN$	Temp. of secondary air at valve unit inlet
$T2\_OUT$	Temp. of secondary air at valve unit outlet
$T\_Rotor-A$	Temp. at rotor inlet
TC	Thermocouple
$TC-IN$	Temp. at test channel inlet
$TC-OUT$	Temp. at test channel outlet
$TC-BEND1$	Temp. upstream of test channel bend
$TC-BEND2$	Temp. downstream of test channel bend
TLC	Thermochromic Liquid Crystal
u	Fluid velocity
(x, y)	pixel coordinates

1. TEST RIG SET-UP

An overview of the rotating test rig concept is given in Figure 1. It consists of a rotor which is supported by two ball bearings.

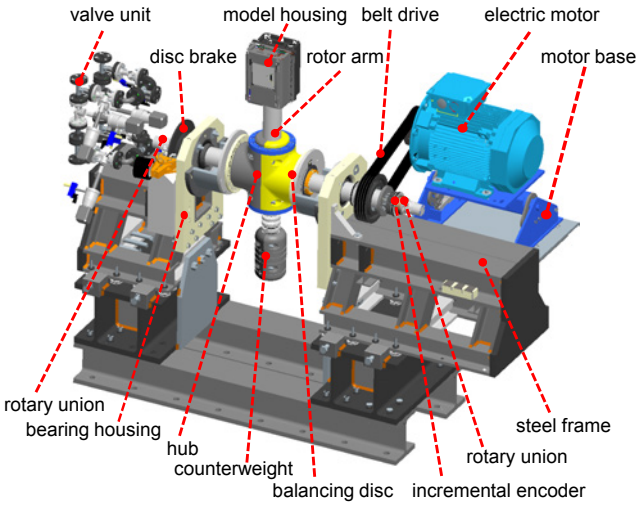

Figure 1. Rotating test rig concept

The rotor is mounted in a steel frame comprised of separate welding assemblies, which can be adjusted in order to align the two bearing housings. The rotor is driven by a 55 kW electric motor via belt drive. The rotation speed can be varied using a frequency converter, which controls the accelerating and decelerating processes.

In case of an emergency a disc brake can be manually activated. During operation the brake caliper is pneumatically released. By opening the brake's pneumatic line, spring forces close the break caliper to stop the rotor within few seconds.

1.1 Rotor

A cross-section view of the rotor is given in Figure 2. The maximum rotor diameter is 2 m. The test model is installed inside an aluminum housing which is mounted at the end of a rotor arm. A counter weight consisting of two half-shells can be mounted at several discrete positions on a counterweight arm. Additional smaller balancing weights will be inserted into grooves of the counterweight for finer balancing. Rotor arm and counterweight arm are clamped on the shaft with a hub consisting of two half-shells. Clamping sets are used to mount the hub, the disc break and the pulley on the shaft.

Pipes are fitted inside the hollow shaft and the hollow rotor arm to supply the test air to the model. The test air is introduced into the shaft via a rotary union (*Deublin 2620-520-252*). A second rotary union at the opposite shaft end supplies cooling air in order to precool the test air pipes inside the shaft and the rotor arm prior to the experiment. For this the supply pipes are made of three integrated pipes, see Figure 3. The central pipe leads the actual test air to the model. The outer pipes contain the cooling air to precool the central pipe. This reduces the warming of the test air on its way to the test model in order to generate a fluid temperature change with a

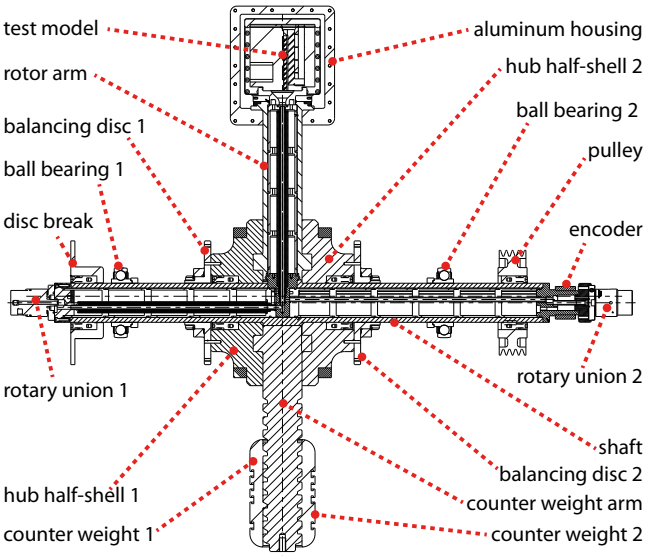

Figure 2. Rotor

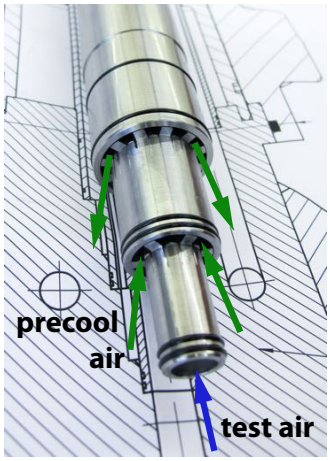

Figure 3. Air supply pipes

steep gradient for the transient experiments.

1.2 Test Model

A dummy test model was designed to conduct preliminary tests. The test model is manufactured out of two Perspex half-shells, into which the cooling channels are milled. Figure 4 shows one half-shell (left) and the complete test model integrated in an aluminum frame (right).

The turbine blade cooling channel configuration consists of an inlet channel with a trapezoidal cross-section, a channel length of 200 mm and a hydraulic diameter of 15 mm. The inlet channel is followed by a U-bend and an outlet channel with a rectangular cross-section and a hydraulic diameter of 20 mm. Suction side and pressure side surfaces are ribbed and coated with TLCs and black paint. The cooling channel geometry is derived from a geometry that has been investigated on a non-rotating test rig by the authors [7].

The ribs are blanked out in post processing as here the heat transfer can not be evaluated with the current evaluation method. This method is based on the assumption of 1D-heat conduction inside a semi-infinite wall. On 3D geometries like rib turbulators this assumption is not applicable. Ryley et al. [8] present an evaluation method combining transient TLC measurements with a finite element analysis. This way they are able to obtain seamless HTC profiles for ribbed channels. Similar evaluation methods may be implemented at a later stage.

A custom-made sensor signal amplifier by *Manner Sensortelemetrie* is mounted to the outside of the test model. Up to 22 thermocouples and up to 6 pressure transducers can be connected to the sensor signal amplifier. This allows to measure the fluid temperature and pressure development at several positions inside the model. Figure 4 shows the custom-made thermocouples type K by *ThermoExpert* positioned along the center line of the channel. The thermocouple sheath is specially enforced to withstand the centrifugal forces.

At the inlet and outlet of the test channel the absolute static pressure at the wall is measured with absolute pressure transducers by *Kulite*. Additionally a differential pressure transducer is applied to measure the pressure loss over the length of the channel directly. The signal amplifier is part of a radio telemetry system which transmits measure data in real-time to an external receiver. The signal is fed to an antenna on the exterior of the model housing via a cable lead-through in the model housing. Also the power to the signal amplifier is supplied via the cable lead-through by a battery pack positioned at the bottom side of the model housing.

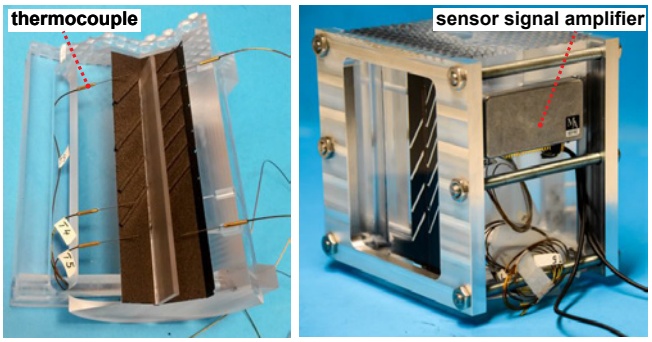

Figure 4. Test model

1.3 Fluid Temperature Change

The transient TLC technique is based on the measurement of TLC color indication times due to a change in fluid temperature. Most non-rotating TLC experiments make use of electric heaters to generate the fluid temperature change and thus obtain the heat transfer from the fluid to the channel walls. However, for rotating experiments the working fluid temperature needs to be lower than that of the channel walls in order to reproduce the correct sense of the buoyancy force. Since the model is at ambient temperature the working fluid needs to be cooled down.

An air compressor (12 bar) together with a recuperator heat exchanger with a controlled LN_2-intake provide a continuous

cooling air flow. With the help of a valve unit (see Figure 5), which controls the air supply to the rotor, the air supply pipes between heat exchanger and valve unit are precooled. This way heat losses in the supply passages can be reduced and the required low temperatures at the inlet of the rotor can be achieved.

The bypass valve unit allows to switch between two separate airflows. It consists of six fast switching valves that can be individually controlled. In the *Default* state both airflows bypass the rotor. In case of power loss or an unwanted drop in the valve control pressure, the valves will adopt this *Default* state.

In the *Tempering* state the secondary airflow with the ambient temperature T2 is lead through the rotor reversed to the actual flow direction to prevent cold air from the precooled internal supply pipes to enter the model. This way the model is tempered to a defined isothermal start temperature prior to the experiment. The experiment starts by switching all six valves simultaneously to the *Experiment* state. Now the primary airflow, the cold test air with the temperature T1, is lead through the precooled pipes to the model in the correct flow direction. Figure 6 depicts the flow paths of the two airflows for the three different states.

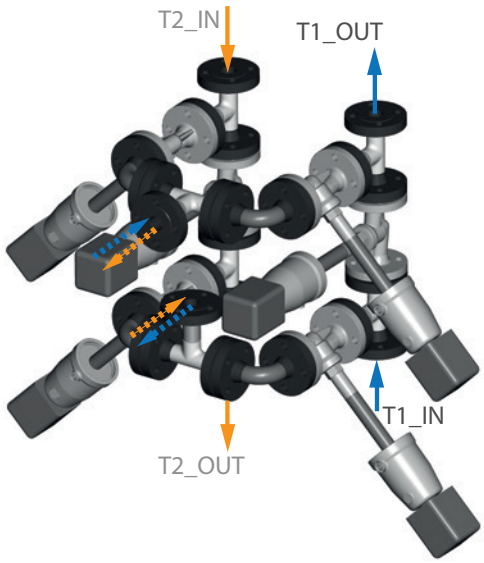

Figure 5. Bypass valve unit

1.4 Stationary Cameras and Strobe Lamps

The TLC colorplay will be captured by color CCD-cameras (*Dalsa 22-2M30-SA*) with a resolution of 1600 x 1200 pixels, a pixel size of 7.4 μm x 7.4 μm, and a sensor size of 11.8 mm x 8.9 mm. *A Zeiss Planar T* ZS* lens with a fixed focal length of 50 mm and a maximum aperture of f/1.4 is used. One camera is installed for each observed surface. The cameras are positioned at a working distance of approx. 1400 mm along the circumference of the rotor together with strobe lamps (Drello Drelloscop 3018 - LE4040/20), see Figure 7.

The model housing can be mounted with a heading angle

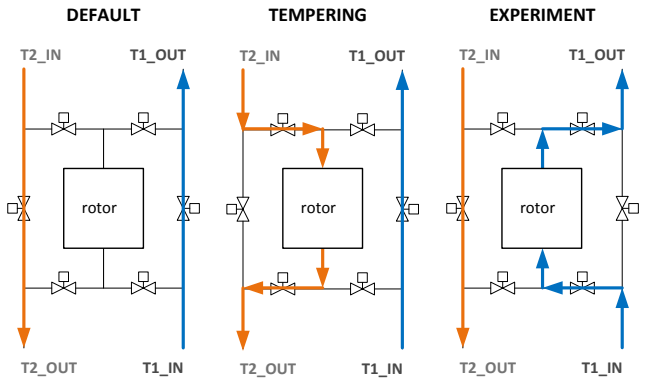

Figure 6. Bypass valve unit scheme

between -30° and +30° at the end of the rotor arm. This allows for an optimal positioning of different turbine blade geometries with respect to the plane of rotation. To ensure a perpendicular view on the observed surfaces, the viewing angle of the cameras (with respect to the plane of rotation) can be varied between -30° and +30° as well.

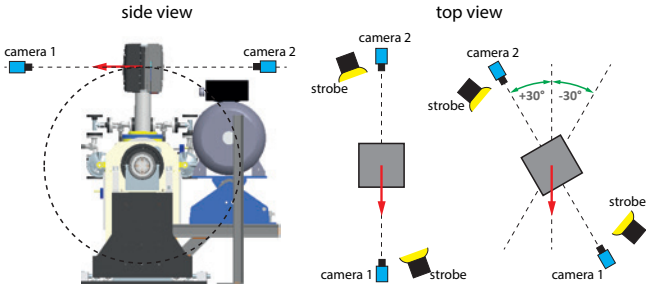

Figure 7. Position of stationary cameras

Cameras and strobe lamps are synchronized with the speed of the rotor by an incremental encoder which is mounted on the rotor shaft. A counter module (National Instruments PXI-6602) evaluates the encoder pulses and generates trigger signals for cameras and strobe lamps. Figure 8 shows the trigger scheme. The encoder provides a zero pulse signal at a predefined angular position. After a specific number of pulses is registered (C1 for camera, C2 for strobe), the counter module generates the respective trigger signal. The experiment is conducted in a darkened room so that the strobe is the only lighting source for the video. Strobe flash durations of 10 μs to 25 μs (full width at half maximum) are short enough to freeze the motion. The exposure time of 100 μs for the camera has to be positioned to comprise the complete strobe flash duration.

1.5 Achievable Test Conditions

The purpose of the rotating test rig is to measure the heat transfer distribution in a scaled test model in order to project these results to real engine dimensions and operating conditions. This can be done when the relevant dimensionless quantities are equal between model test and real engine conditions. A dimensional analysis yields the relevant dimensionless quan-

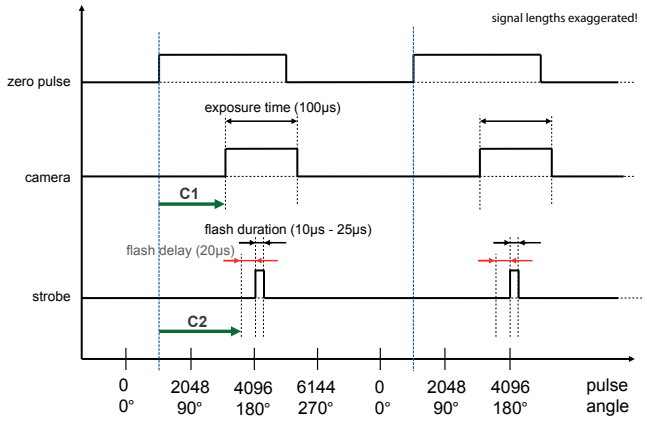

Figure 8. Trigger scheme

tities for rotating cooling channels and reveals that the heat transfer mainly depends on the following quantities:

$$\mathrm{Nu} = f\,\{\mathrm{Re}, \mathrm{Ro}, \mathrm{Bo}, \mathrm{Pr}, \mathrm{Ma}\} \tag{1}$$

The Nusselt number Nu describes the convective heat transfer between fluid and channel wall. The hydraulic diameter d_h is used as characteristic length.

$$\mathrm{Nu} = \frac{h\ d_h}{\lambda_f} \tag{2}$$

The Reynolds number Re is the ratio of inertia forces to viscous forces. As the fluid velocity u inside the channel cannot be measured directly, the Reynolds number is calculated using the massflow rate $\dot{m}$ and the channel cross-section area A.

$$\mathrm{Re} = \frac{\rho\ u\ d_h}{\eta} = \frac{\dot{m}\ d_h}{A\ \eta} \tag{3}$$

The rotation number Ro is the ratio of Coriolis forces to inertia forces.

$$\mathrm{Ro} = \frac{\Omega\ d_h}{u} \tag{4}$$

The buoyancy number is the ratio between buoyancy forces and inertia forces and is relevant for inhomogeneous fluid density distributions.

$$\mathrm{Bo} = \frac{\Delta\rho}{\rho}\ \mathrm{Ro}^2\ \frac{R}{d_h} \tag{5}$$

Air is used as cooling fluid for both model test and real engine operation, resulting in a similarity regarding the Prandtl number Pr. For the relatively low flow velocities (Ma<0.3) the similarity in Mach number can be neglected.

Figure 9 shows the estimated range of test conditions that can be achieved for a channel with a hydraulic diameter of $d_h = 15mm$. The depicted ranges encompass rotational speeds between 300 rpm and 900 rpm, mass flow rates between 2 g/s and 16 g/s, and air pressures of up to 7.5 bar.

However, buoyancy number and rotation number cannot be set completely independent from each other. For a given rotation number the buoyancy number can be changed by varying the density ratio, which is determined by the temperature difference between wall and cooling fluid. However, these temperatures have to be adjusted to the applied TLC type in order to obtain suitable indication times.

For a higher flexibility in temperature and TLC type combinations, the Perspex model can be preheated before the experiment. Additionally, the application of mixtures of different TLC types has been investigated by the authors [9]. Using TLC mixtures, multiple indications are obtained in a single experiment. This way the temperature combination can be set more independently from the operating range of the TLCs.

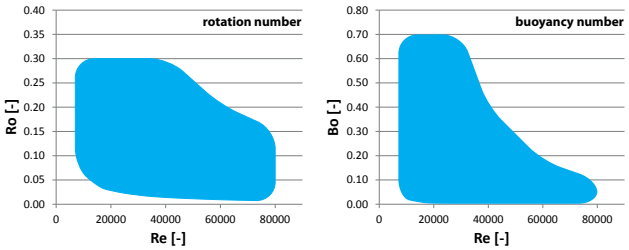

Figure 9. Range of achievable rotation numbers (left) and buoyancy numbers (right)

1.6 Preliminary Tests

Preliminary tests have been conducted to test several measurement aspects. A stationary (i.e. non-rotating) test rig was set-up to investigate the required fluid temperature change. A rotating aluminum disc was used to validate the trigger concept and to evaluate motion blur effects.

1.6.1 Stationary Test Rig

The stationary test rig mainly consists of an aluminum model housing, a simplified rotor arm and a simplified rotor shaft. While the aluminum housing has the same dimensions as the actual housing, the rotor arm, shaft and the internal air supply pipes are shortened. However, all diameters of rotor, shaft and internal pipes have been maintained.

The rig is used to test the precooling of the internal air supply passages and to evaluate the fluid temperature change that can be achieved using the bypass valve unit. Figure 10 shows the rig together with the bypass valve unit and the valve control system.

For the preliminary tests the actual air supply system was not available. However, the infrastructure of an existing test rig including a regenerative heat exchanger could be adapted. An overview of the setup is given in Figure 11.

Compressed air is used to provide three separate air flows for the test rig. One air flow (orange) is taken directly after the air dryer and has approximately ambient temperature. This is the secondary air flow which is connected to the bypass valve unit and used to temper the model in the *Tempering* phase. The remaining air is split to either go through or bypass the heat exchanger. These two air streams are then again

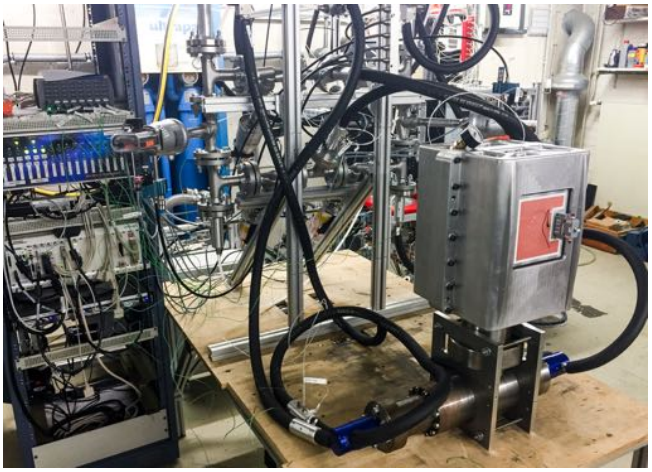

Figure 10. Stationary test rig

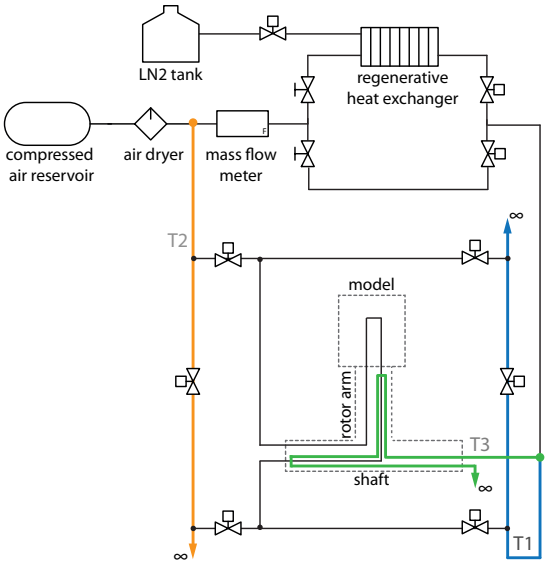

Figure 11. Stationary test rig scheme

mixed together in a controlled ratio using two control valves. This is necessary to ensure a constant exit temperature, as the regenerative heat exchanger changes its exit temperature during operation.

The resulting airflow is split again into two streams. The first one is the primary test airflow (blue) and connected to the bypass valve unit. The second stream (green) is directly connected to the second rotary union and used to precool the internal air supply pipes inside the shaft and the rotor arm during the *Tempering* phase. During the *Experiment* phase this airflow is cut off in order to measure the mass flow rate of the primary airflow with the mass flow meter upstream of the heat exchanger.

Figure 12 shows the thermocouple measurement positions for the preliminary tests. All thermocouples are of type K and positioned in the fluid region. For the valve unit the sensors were connected to a MEASUREpoint precision measurement instrument by *data translation*. The thermocouple measurements inside the model were obtained by the sensor signal amplifier. Both systems have integrated cold junction compensation.

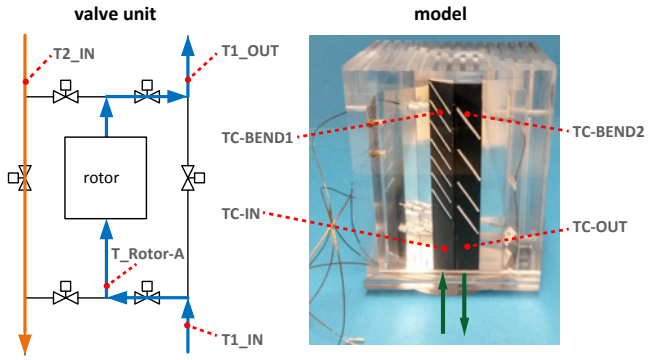

Figure 12. Thermocouple positions

1.6.2 Rotating Disc Test Rig

The rotating disc test rig consists of an aluminum disc with an overall diameter of 300 mm that is directly mounted on the shaft of an electric motor, see Figure 13.

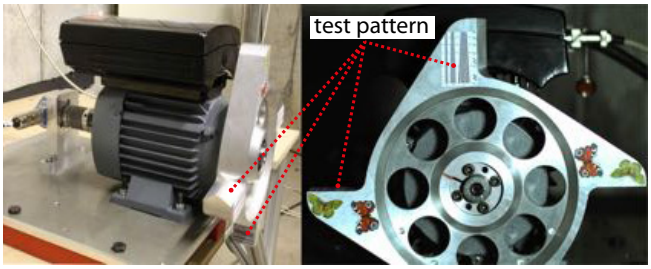

Figure 13. Rotating disc test rig

The rotational speed can be set to values of up to 4800 rpm by a frequency converter. Test patterns on several positions on the disc allow viewing angles between 0° (along the plane of rotation) and 90° (view perpendicular to the plane of rotation), see Figure 14.

At the distance of 1400 mm between camera and test pattern an image resolution of approx. 5 pixel/mm was obtained. An incremental encoder with a resolution of 8192 impulses per revolution was mounted on the rear end of the motor shaft. The tests to evaluate the triggering of camera and strobes have been conducted at a frequency of 15 Hz, the maximum frequency for the test rig.

To evaluate possible motion blur effects, tests have been conducted at comparable circumferential speeds, see Table 1. However, limited by the rotational speed of the motor, the maximum circumferential speed of RotRig could not be fully achieved.

Motion blur depends on the relative motion between captured object and camera during the exposure. It also depends on the working distance D, the focal length f, the pixel size and camera sensor size. Figure 15 shows that the effect of motion blur is clearly evident for a relative motion parallel to

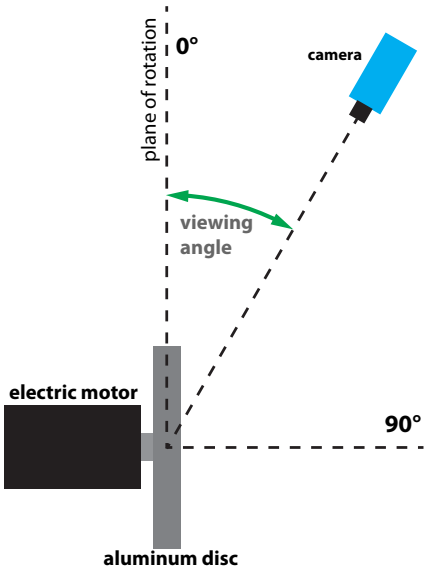

Figure 14. Test set-up for rotating disc

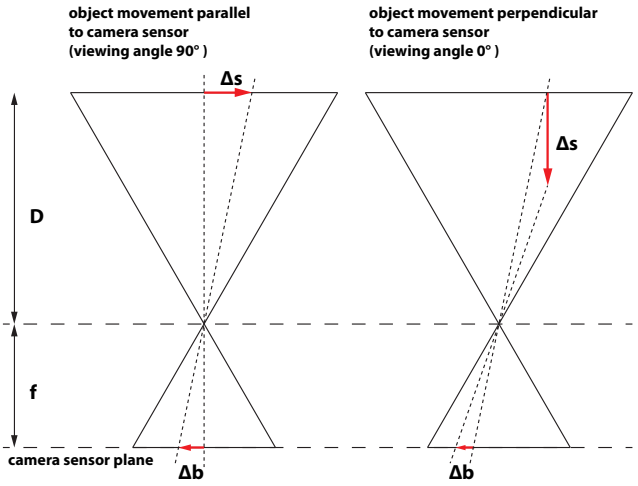

Figure 15. Cause of motion blur

Table 1. Test conditions for preliminary rotating tests

		Prelimin. Test	
	Concept	Trigger	Blur
rotational speed [rpm]	900	900	4800
frequency [Hz]	15	15	80
radius [mm]	750	125	125
circumf. speed [m/s]	70.7	11.78	62.8

the camera sensor (viewing angle 90° on plane of rotation), as the motion causes a shift of the projected image on the camera sensor.

For a relative motion perpendicular to the camera sensor (viewing angle along plane of rotation) the effect is significantly smaller. Here an object motion towards the camera causes the size of the projected image on the camera sensor to increase during exposure. Motion blur is therefore also dependent on the distance from the image center, with increasing blur towards the image borders.

The default viewing angle for the test concept is 0° with respect to the plane of rotation. For this viewing angle the expected maximum shift of the image on the sensor has been calculated. At the working distance of $D = 1400\,\text{mm}$, a camera sensor height of $h = 8.9\,\text{mm}$ and a focal length of $f = 50\,\text{mm}$ an object with the height of $H = 250\,\text{mm}$ can be captured. At the maximum rotation speed of 900 rpm the model travels a distance of $\Delta s = 1.77\,\text{mm}$ at the mean model radius of $R = 750\,\text{mm}$ during the exposure time of $t = 25\,\mu\text{s}$. This results in a maximum shift of the image on the camera sensor of $\Delta b = 5.6\,\mu\text{m}$ (at the border of the image) which is below the pixel size of $7.4\,\mu\text{m}$. Hence, no significant motion blur is expected for a viewing angle along the plane of rotation.

2. RESULTS OF PRELIMINARY TESTS

2.1 Fluid Temperature Change

The result of a test with a test air mass flow rate of 7.5 g/s is given in Figure 16. The diagrams show the switching moment from *Tempering* to *Experiment* at $t = 0\,\text{s}$. After 66 s the valve unit was switched back again into the *Tempering* state. It can be seen that the valve unit was not completely precooled before the experiment. The test air enters the valve unit at -50 °C (T1-IN) and leaves the unit with -30 °C (T1-OUT) during the *Tempering* phase. This is due to the fact that the regenerative heat exchanger can only be operated for approx. 20 min until it has to be cooled down again with LN_2. This time span is too short to establish a precooled steady state for the valve unit and the internal pipes of the rotor. However, as the actual designed recuperator heat exchanger can be operated continuously for a few hours this will not be a problem for the test rig concept.

During the *Tempering* phase the secondary airflow with a temperature of +22 °C (T2-IN) is lead through the rotor and model. At the measuring point T_ROTOR-A the temperature is obtained as this airflow leaves the rotor. After switching the valves into the *Experiment* state, the flow direction in the rotor is reversed. Now the primary air flow is lead through the rotor and through the model. Also at the measuring point T_ROTOR-A the temperature of the fluid entering the rotor is obtained. Here a sudden temperature change from +20 °C to -10 °C is achieved.

The bottom part of Figure 16 shows the fluid temperature histories at four different thermocouple positions along the test channel. At the channel inlet (TC-IN) a temperature drop from +22 °C to +8.6 °C can be observed. Due to heat loss inside the model the temperature drops only to +10.6 °C at the channel outlet (TC-OUT).

With this temperature change inside the model, experiments with TLC indication temperatures of approx. +13 °C would be possible. We expect to achieve higher temperature drops with the actual cooling air supply system, which provides even lower temperatures and extended precooling time

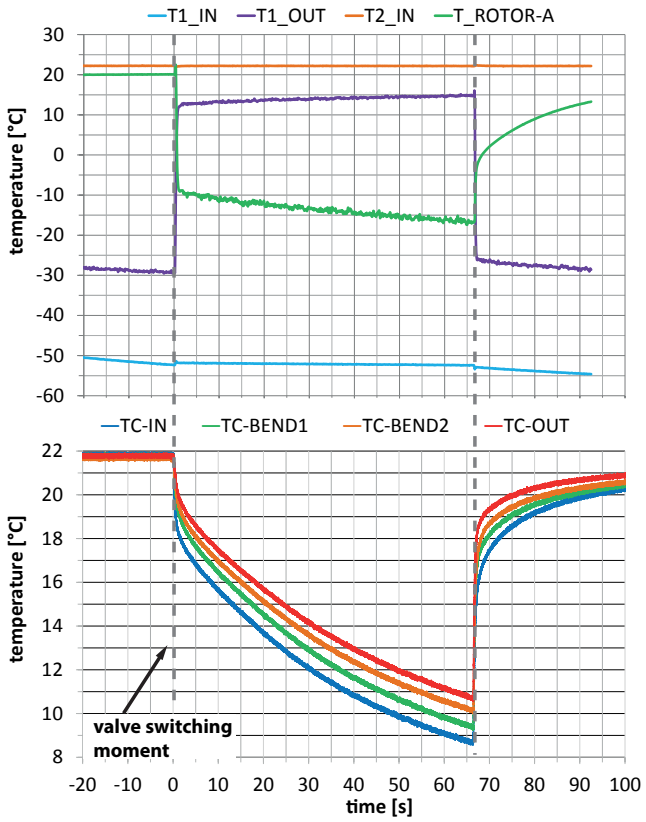

Figure 16. Temperature change, valve unit (top), model (bottom)

spans. The application of TLCs with indication temperatures of -10 °C to +15 °C is planned to cover the needed buoyancy range. Furthermore, the possibility to use TLC mixtures to get multiple indications in a single experiment have been investigated in previous studies by the authors [9].

2.2 Rotating Disc Test

2.2.1 Flash Stability

The transient TLC method is based on the measurement of indication times. A reliable approach is to evaluate the intensity histories of the video and to determine the time at which the intensity reaches its maximum. This is done for each RGB-color channel and for each video pixel separately. For this method a stable lighting source is needed.

Figure 17 shows the measured flash intensity of the strobe operating at its highest energy level of 7.5 J per flash and at a frequency of 15 Hz. This frequency corresponds to the maximum rotational speed of 900 rpm. For lower rotational speeds the strobe frequency reduces accordingly.

The depicted values are averaged intensity values extracted from a video of a gray target region of 200 x 150 pixels on the aluminum disc. For this evaluation the color video was converted to an 8 bit intensity gray-scale video. The aperture of the lens was adjusted to obtain values in the mid-range of the gray scale. It can be seen that for this setting the strobe needs a warm-up time of approximately 120 s to reach a stable level.

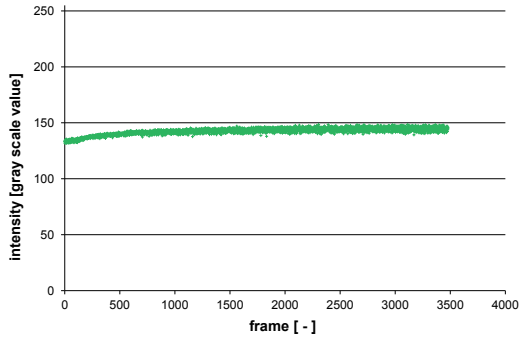

Figure 17. Flash stability (flash energy 7.5 J/flash)

Experiments should only be conducted with a warmed-up strobe.

The standard deviation of the measured intensity for the warmed up strobe was determined to 1.77 (gray scale value) or 1.22 % with respect to the mean value. This is stable enough for almost all TLC evaluations. However for different strobe settings (lower energy levels, lower frequency) the relative standard deviation can increase to values of up to 3.70 %. This variation in flash intensity will be noticeable as a slight flickering in the resulting video.

A means to compensate the variation in flash intensity is to normalize each frame with a reference intensity, see Equation 6:

$$I_j^*(x,y) = \frac{E_{ref}}{E_j} I_j(x,y) \quad ; j = 1...N \tag{6}$$

For this method a gray reference area has to be visible in the video. For each video-frame $I_j(x,y)$ the intensity E_j has to be determined by averaging the intensity of a group of pixels in this target area. One intensity value has to be set as reference value, for example the intensity of the first frame $E_{ref} = E_1$. The normalization factor for each frame is the ratio of E_{ref} and E_j. It is important to avoid oversaturation for every pixel used for the calculation of E_j.

2.2.2 Motion Blur

Figure 18 shows the comparison of the captured test patterns between non-rotating disc (left) and rotating disc (right). The images are cropped sections of the original images with a size of 1.92 megapixels.

It can be seen that for a viewing angle of 0°, as expected, no significant motion blur occurs. At a viewing angle of 30°, a slight blur at high-contrast edges is visible. However a TLC experiment with this viewing angle could still be evaluated.

Viewing angles larger than 30° are not planned for tests. However, for a clear demonstration of the motion blur effect, also a viewing angle of 90° is depicted. The resulting image appears significantly less sharp. The TLC experiment with this viewing angle could be evaluated but would also yield blurred results.

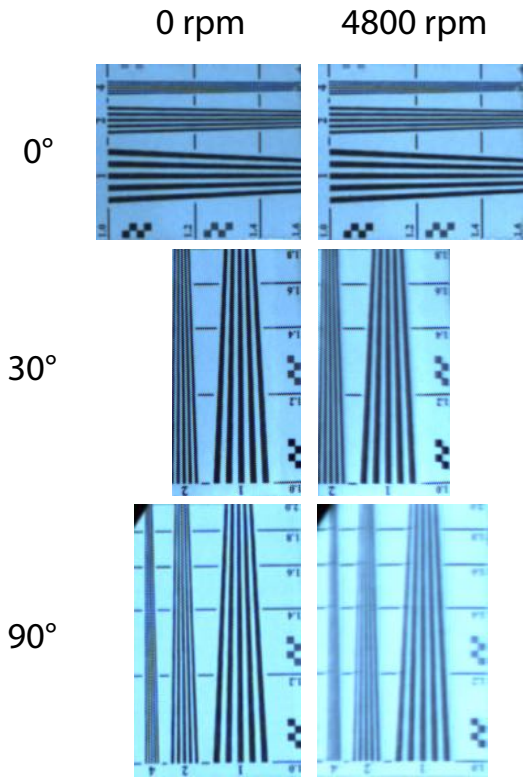

Figure 18. Captured test patterns for non-rotating disc (left) and rotating disc (right)

3. CONCLUSION

In this paper the design of a new rotating test rig has been presented. Preliminary tests have been conducted to validate that the required fluid temperature change for the transient TLC method can be achieved. The air supply system of a existing test rig has been adapted to provide three separate airflows for these preliminary non-rotating tests. A bypass valve unit controls the air supply to the test model and allows the tempering of the test model while the air supply pipes are precooled.

The triggering concept for the camera and strobe lamp has been validated using a rotating aluminum disc. Also preliminary tests regarding motion blur have been conducted, with the conclusion that for low viewing angles motion blur effects can be neglected.

ACKNOWLEDGMENTS

The investigations were conducted as part of the joint research programme COORETEC-turbo (AG Turbo 2020) in the frame of AG Turbo. The work was supported by the Bundesministerium für Wirtschaft und Energie (BMWi) as per resolution of the German Federal Parliament under grant number 03ET2013D. The authors gratefully acknowledge AG Turbo, ALSTOM Power and MTU Aero Engines for their support and permission to publish this paper. The responsibility for the content lies solely with its authors.

REFERENCES

[1] J. H. Wagner, B. V. Johnson, and T. J. Hajek. Heat Transfer in Rotating Passages With Smooth Walls and Radial Outward Flow. *J. Turbomach.*, 113(1):42–51, 1991.

[2] J. H. Wagner, B. V. Johnson, and F. C. Kopper. Heat Transfer in Rotating Serpentine Passages With Smooth Walls. *J. Turbomach.*, 113(3):321–330, 1991.

[3] M. F. Blair, J. H. Wagner, and G. D. Steuber. New applications of liquid–crystal thermography in rotating turbomachinery heat transfer research. *ASME, International Gas Turbine and Aeroengine Congress and Exposition, 36th, Orlando, FL, June 3-6, 1991. 11 p.*, 1991.

[4] W. D. Morris. A rotating facility to study heat transfer in the cooling passages of turbine rotor blades. *Proceedings of the Institution of Mechanical Engineers, Part A: Journal of Power and Energy 1990-1996 (vols 204-210)*, 210(11):55–63, 1996.

[5] R. Davenport. The Benefits of a Rotating Rig for Research into Advanced Turbine Cooling Systems: RTO MEETING PROCEEDINGS 8. *RTO Applied Vehicle Technology Panel (AVT) Symposium, Toulouse, France*, 1998.

[6] R. Poser and J. von Wolfersdorf. Transient liquid crystal thermography in complex internal cooling systems. *VKI Lecture Series - Internal Cooling in Turbomachinery, von Karman Institute for Fluid Dynamics*, (VKI LS 2010-05), 2010.

[7] C. Waidmann, R. Poser, J. von Wolfersdorf, M. Fois, and K. Semmler. Investigation of Heat Transfer and Pressure Loss in an Engine-similar Two-pass Internal Blade Cooling Configuration. *10th European Conference on Turbomachinery Fluid Dynamics and Thermodynamics, Lappeenranta, Finland*, pages 1051–1063, 2013.

[8] J. C. Ryley, M. McGilvray, and D. R. H. Gillespie. Calculation of Heat Transfer Coefficient Distribution on 3D Geometries From Transient Liquid Crystal Experiments. In *ASME Turbo Expo 2014: Turbine Technical Conference and Exposition*, page V05BT14A019, Monday 16 June 2014.

[9] C. Waidmann, R. Poser, and J. von Wolfersdorf. Application of Thermochromic Liquid Crystal Mixtures for Transient Heat Transfer Measurements. *10th European Conference on Turbomachinery Fluid Dynamics and Thermodynamics, Lappeenranta, Finland*, pages 685–696, 2013.